doi:10.1016/j.jmb.2005.10.012 J. Mol. Biol. (2005) 354, 1028–1042

JMB

Available online at www.sciencedirect.com

SCIENCE DIRECT®

ELSEVIER

Protein Interactions and Misfolding Analyzed by AFM Force Spectroscopy

Chad McAllister[1], Mikhail A. Karymov[1,2], Yoshiko Kawano[1] Alexander Y. Lushnikov[1,2], Andrew Mikheikin[2] Vladimir N. Uversky[3,4] and Yuri L. Lyubchenko[1,2]*

[1]*School of Life Sciences, Arizona State University, Tempe, AZ 85287-4501, USA*

[2]*Department of Pharmaceutical Sciences, University of Nebraska Medical Center, Omaha, NE 68198, USA*

[3]*Center for Computational Biology and Bioinformatics Department of Biochemistry and Molecular Biology, Indiana University School of Medicine Indianapolis, IN 46202, USA*

[4]*Institute for Biological Instrumentation, Russian Academy of Sciences, Pushchino Moscow Region 142290 Russian Federation*

**Corresponding author*

Protein misfolding is conformational transition dramatically facilitating the assembly of protein molecules into aggregates of various morphologies. Spontaneous formation of specific aggregates, mostly amyloid fibrils, was initially believed to be limited to proteins involved in the development of amyloidoses. However, recent studies show that, depending on conditions, the majority of proteins undergo structural transitions leading to the appearance of amyloidogenic intermediates followed by aggregate formation. Various techniques have been used to characterize the protein misfolding facilitating the aggregation process, but no direct evidence as to how such a conformational transition increases the intermolecular interactions has been obtained as of yet. We have applied atomic force microscopy (AFM) to follow the interaction between protein molecules as a function of pH. These studies were performed for three unrelated and structurally distinctive proteins, α-synuclein, amyloid β-peptide (Aβ) and lysozyme. It was shown that the attractive force between homologous protein molecules is minimal at physiological pH and increases dramatically at acidic pH. Moreover, the dependence of the pulling forces is sharp, suggesting a pH-dependent conformational transition within the protein. Parallel circular dichroism (CD) measurements performed for α-synuclein and Aβ revealed that the decrease in pH is accompanied by a sharp conformational transition from a random coil at neutral pH to the more ordered, predominantly β-sheet, structure at low pH. Importantly, the pH ranges for these conformational transitions coincide with those of pulling forces changes detected by AFM. In addition, protein self-assembly into filamentous aggregates studied by AFM imaging was shown to be facilitated at pH values corresponding to the maximum of pulling forces. Overall, these results indicate that proteins at acidic pH undergo structural transition into conformations responsible for the dramatic increase in interprotein interaction and promoting the formation of protein aggregates.

Keywords: protein misfolding; intermolecular interaction; force spectroscopy; AFM; amyloids

Introduction

Protein folding is a key step for creating functional proteins during peptide synthesis on ribosomes within cells. However, some of the polypeptide chains undergo the misfolding path and form non-functional aggregates. Initially, the formation of aggregates was linked with various neurodegenerative disorders, including Alzheimer's, Parkinson's and Huntington's diseases. In each of these pathological states, a specific protein or protein fragment changes from its natural, soluble form into insoluble aggregates that accumulate in a variety of organs and tissues.[1–7] Application of direct imaging techniques such as electron microscopy and atomic force microscopy (AFM) showed

Abbreviations used: AFM, atomic force microscopy; ANS, 8-anilino-1-naphthalene sulfonic acid.

E-mail address of the corresponding author: ylyubchenko@unmc.edu

that aggregates were often long filaments that were several nanometers in diameter.[8,9] High-resolution electron microscopy and AFM studies revealed a periodic structure along the amyloid filaments.[6] Recent data, however, suggests that the ability to form amyloid filaments is not restricted to the proteins associated with these diseases, but rather is intrinsic to all polypeptides.[2,7–10]

A great deal of effort has been made towards understanding the aggregation of amyloid β-peptide (Aβ). This peptide consists of 39–43 amino acid residues and is the principal component of amyloid plaques in the brains of Alzheimer's patients.[11] Aβ peptide can aggregate spontaneously. Its *in vitro* aggregation has been studied extensively and it has been shown that the rate of aggregation is very fast at acidic pH in comparison with neutral pH.[12] Models explaining the aggregation of Aβ peptide utilize β-sheet structure formation as the initial step followed by the aggregation of peptides *via* interaction between the β-sheets. Recent solid-state NMR observations revealed such an interprotein interaction and allowed elucidation of the structure of the Aβ peptide within the aggregate.[13–15]

α-Synuclein is a 140 amino acid residue presynaptic protein, which is a typical member of the family of natively unfolded proteins, and whose fibrillation was also studied extensively.[16,17] This protein has been estimated to account for as much as 0.5–1% of the total protein in soluble cytosolic brain fractions. It has been emphasized that the misfolding and deposition of α-synuclein might be involved in the molecular mechanisms underlying Parkinson's disease and related neurodegenerative brain amyloidoses.[18–23] The fibrillogenesis of α-synuclein has been studied extensively using various techniques.[24–31] In particular, accumulated data suggest strongly that the formation of a partially folded intermediate (possessing the major characteristics of the pre-molten globule) represents the critical first step of α-synuclein fibrillogenesis. This partially folded intermediate can be stabilized by numerous factors, including high temperatures and low pH.[32]

Lysozyme is known to be involved in an amyloid-related human disorder, hereditary systemic amyloidoses,[33] in which the disease is associated with single-point mutations in the lysozyme gene, and fibrils are deposited widely in tissues. Wild-type human lysozyme and its two amyloidogenic variants have been found to form a partially folded state at low pH.[34] This state was characterized by extensive disruption of tertiary interactions and partial loss of secondary structure. Incubation of these proteins at pH 2.0 resulted in the formation of large numbers of fibrils over several days of incubation.[34] The amyloidogenic mutant proteins were significantly less stable than the wild-type protein, leading to higher populations of the partially unfolded intermediate and thus greater propensity to form fibrils. A number of homologous proteins, including equine lysozyme,[35] hen egg-white lysozyme,[36] and α-lactalbumin[37] were shown to assemble into amyloid-like fibrils at acidic pH and elevated temperatures. Particularly, for hen egg-white lysozyme, it has been shown that fibril formation is promoted by low pH and temperatures close to the midpoint temperature for protein unfolding. At the optimal conditions for fibril formation (pH 2.0, 57 °C), static light-scattering measurements revealed the formation of fibrils after a lag time of around 48 h. This nucleation step was assumed to involve a change in the conformation of individual lysozyme molecules.[36]

The prevalent structural feature of amyloid filaments formed by all proteins studied so far is the presence of extensive β-sheet structure. It is assumed that the formation of β-sheet structure is a critical step for fibrillation or formation of aggregates with other morphologies; however, there is no direct evidence for the link between the protein misfolding and the increase of the interprotein interaction leading to the aggregation. The effect of different environmental factors on the aggregation rates of different proteins (including Aβ) has been studied intensively; however, nothing is currently known about the strength of the direct physical interaction between the protein molecules under the conditions favoring aggregation. Here, we monitored directly the strength of the interprotein interaction depending on the protein conformation for the first time. We studied three proteins of different sizes and origins, Aβ (1-40) peptide, α-synuclein and lysozyme. Proteins were anchored on the mica surface and the AFM probe, and the interaction between such anchored molecules was measured after bringing them together by approaching the tip to the surface. The intermolecular interaction was characterized by the pull-off force required to dissociate the complex formed during the approach cycle.[38] The data obtained show that the interaction between all the proteins increases sharply with a decrease in pH. AFM imaging showed that at pH values corresponding to maximum interprotein interaction, the rate of protein aggregation increases dramatically. The comparison of the AFM data with a conformational analysis of the Aβ-peptide and α-synuclein performed using CD spectroscopy showed that the increase in the protein–protein interaction measured by AFM is due to a conformational transition in the corresponding protein leading to the formation of an ordered structure with an elevated content of β-sheet conformation.

Results

Amyloid β peptide

To achieve the goal of this work and to measure the interprotein interactions, we used the AFM approach. This technique requires proteins to be anchored to the substrate surface and the AFM tip. We used the approach in which protein was covalently linked to amino-functionalized mica

and Si_3N_4 AFM probes *via* glutaraldehyde crosslinking.[39] This technique or similar approaches utilizing longer spacers between the protein and surfaces are quite typical for force spectroscopy analyses.[40] We have shown that glutaraldehyde crosslinked Aβ molecules are accessible to anti-Aβ antibodies in separate force spectroscopy analyses (data not shown). Using the functionalization protocol developed, we were able to obtain a fairly uniform coverage of the surface with the protein (the data for Aβ peptide are shown in Supplementary Data, Figure S1); however, force curves were taken at 80–125 different locations on the surface in order to account for any heterogeneity in the coverage of the protein on the mica surface.

A monomeric form of protein immobilized on the surface prior the force spectroscopy studies is required for the force spectroscopy studies. Monomeric fraction of the protein solution can be obtained by gel-filtration chromatography or sedimentation studies, but the aggregates can form during the relatively long immobilization procedure. Therefore, all morphologies are immobilized on the tip and the substrate surfaces. To avoid this complication, we used an approach based on the known fact that protein aggregation is very inefficient or does not occur at all at alkaline pH. According to published data,[41] spontaneously formed aggregates of the amyloid β peptides are not stable at pH 10 and can dissociate during incubation overnight. So, if the sample containing a mixture of monomers and aggregated forms of the protein is anchored to the surface, during incubation in alkaline solutions aggregates dissociate and non-covalently bound molecules go away from the surface. Note that under our surface functionalization conditions, the distance between active groups on the surface (initially amines) is ca 10–20 nm,[42,43] suggesting that multiple bonding of the same complex with the size of even 10 nm is quite improbable. This suggests that predominantly monomeric forms of the protein remain on the surface. This assumption is in line with direct AFM imaging of the sample. According to Supplementary Data, Figure S1, the samples were homogeneous. To ensure the homogeneity of immobilized samples, they were imaged with AFM before the pulling experiments.

The protein molecules anchored to the mica surface and to the AFM tip were brought into contact, after which the strengths of the complexes formed were measured by retracting the tip from the surface. Figure 1 shows a set of the force–distance curve obtained at various pH values. The attractive force was measured as the pull-off force (arrow) of the retraction curve, which is the force required to rupture any attractive interactions between molecules on the tip and molecules on the surface. Only the pull-off forces of distinct peaks typical for the single-molecule interaction events as shown in the Figure were used in the measurements.

The data in Figure 1(a) show a typical force curve for the sample probed at pH 9.8. The rupture force in the range of 100 pN is typical for the Aβ–Aβ interaction under these conditions. The results obtained for a series of measurements are shown as histograms inset into this Figure. Similar data were obtained for experiments performed at pH 7.0, pH 5.1, pH 3.7, pH 2.0, and pH 1.0 (data are shown in Figure 1(b)–(f), respectively). Similar to Figure 1(a), the data accumulated for a set of approach–retraction cycles measured at each

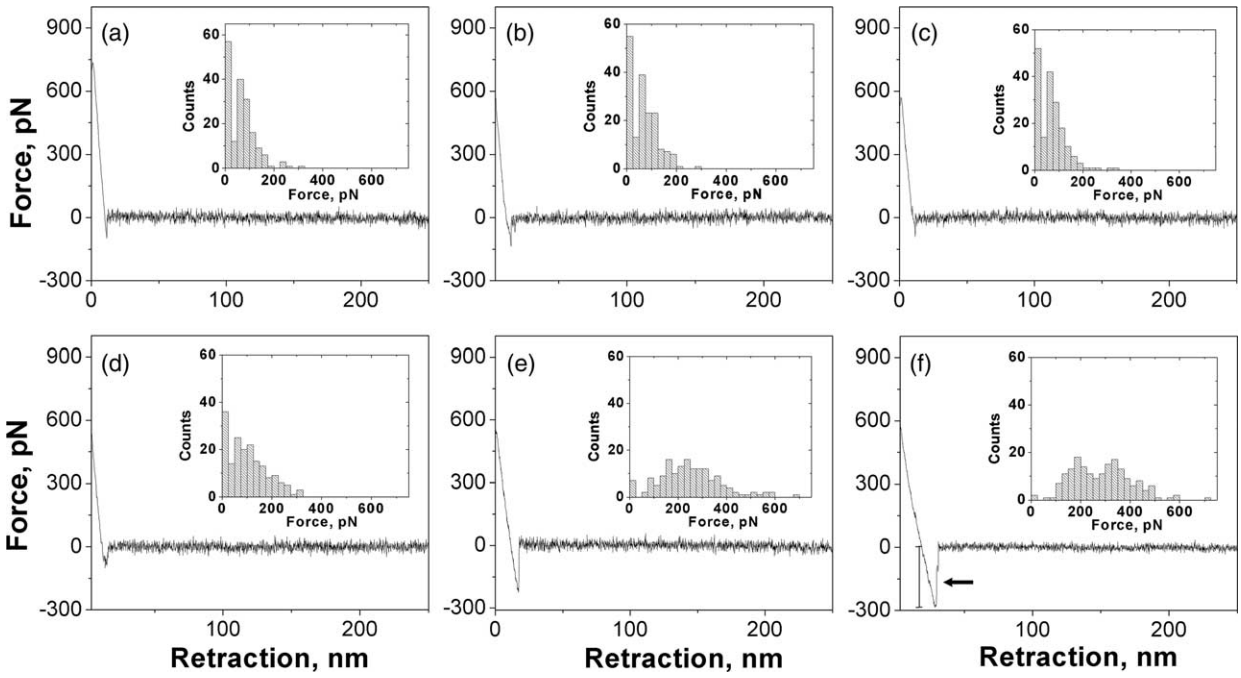

Figure 1. Typical force curves and histograms summarizing all force curves taken at (a) pH 9.8, (b) pH 7.0, (c) pH 5.1, (d) pH 3.7, (e) pH 2.0, and (f) pH 1.0.

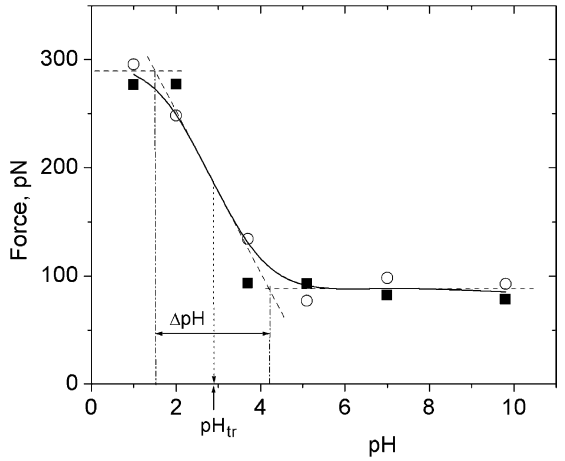

Figure 2. The mean pull-off force plotted as a function of pH for two independent trials (filled squares and open circles). The continuous line represents a sigmoidal fit to the average of the two data sets. Broken lines on this transition curve explain how the width of the transition (ΔpH) and the transition point (pH$_{tr}$) were measured.

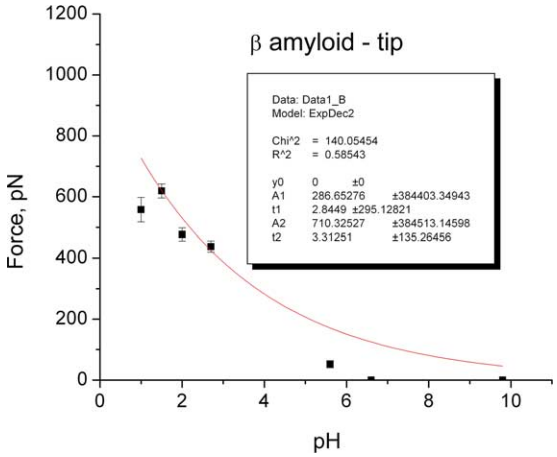

Figure 3. The mean pull-off force plotted as a function of pH for amyloid β peptide immobilized on the surface and the AFM tip terminated with OH groups. The continuous line represents an exponential fit to the data points. The error bars on each datum point (mean force values) correspond to the standard error of the mean (SEM) calculated from the entire set of pull-off forces.

pH value are shown as histograms inset into each force plot. The data indicate that the protein–protein interaction is relatively small between pH 9.8 and pH 7.0 (92 pN and 93 pN, respectively). A strong increase in the rupture forces is observed at pH <3.7 achieving a maximum at pH 1.0 accompanying the formation of multiple interactions between the tip and surface.

The mean pull-off forces as a function of pH are plotted in Figure 2. Different symbols correspond to two independent experimental data sets, and the pH dependence of the rupture force is interpolated by a smooth curve using both data sets. This graph illustrates the attractive force between Aβ molecules and exhibits a sharp sigmoidal pH-dependence, increasing dramatically over a narrow range of pH values (3–4). The averaged value of the pH-dependent increase in the rupture force for Aβ molecules was approximately 200 pN. Such a sharp pH-dependence of the rupture forces suggests that a decrease in pH induces considerable conformational changes in the Aβ-peptide. The data for control experiments in which the peptide immobilized on the surface was probed with the tip with no peptide in the same pH range are shown in Figure 3. The rupture forces increase monotonously with pH with no S-type dependence as observed for peptide–peptide interaction.

The hypothesis on the pH-induced protein structural transition was tested using far-UV CD spectroscopy as an approach for characterizing the secondary structure of the peptide. The same protein batch was used for CD spectroscopy and AFM. Figure 4(a) represents the far-UV CD spectra recorded over a broad range of pH values. The spectra measured between pH 11.4 and pH 5.8 are very similar and indicate little, if any, α-helix or β-sheet structure present in Aβ. In fact, these spectra show characteristic minima in the vicinity of 200 nm and the absence of bands around 210–230 nm; i.e. their shape is typical of an essentially unfolded polypeptide chain. With pH decreasing below 5.8, the inversion of the band at 200 nm from negative to positive occurs concomitantly with an increase in the negative intensity around 220 nm, reflecting the pH-induced formation of ordered secondary structure. Furthermore, the shape of the spectra measured at acidic pH (1–3) is indicative of a β-sheet structure, which is characterized by a typical broad minimum in the vicinity of 220 nm, a positive peak at ∼197 nm, and an intersection point at about 210 nm. The relative β-sheet content as a function of pH can therefore be determined by plotting the ellipticity value of the band at 220 nm against pH (Figure 4(b)). This plot reveals a strong pH-dependence for Aβ secondary structure, where protein, having little or no β-sheet structure at pH greater than 6, possesses a cooperative increase in β-sheet content below this pH value. Most striking is the fact that this sigmoidal dependence is the same as that observed for the increasing attractive force between Aβ molecules with decreasing pH.

These data suggest that aggregation is more favorable under acidic conditions. This conclusion is supported by numerous observations on the effect of pH on aggregation of Aβ molecules by Stine *et al*.[12] Similar to those findings,[12] we observed the formation of long fibrils with 1–40 Aβ peptide (Supplementary Data, Figure S2).

Alpha synuclein

The same experimental approach was utilized to study the pH-dependence of rupture forces between α-synuclein molecules. A series of the

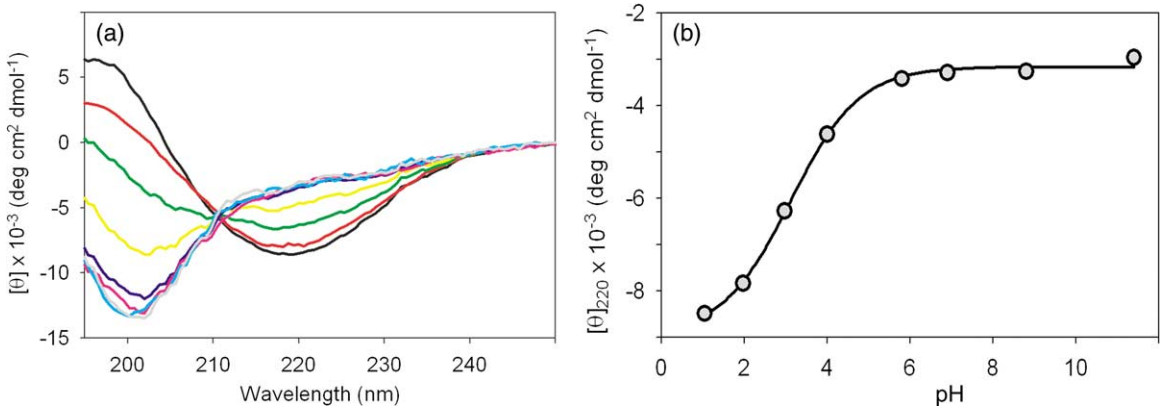

Figure 4. (a) The circular dichroism (CD) spectra for a range of pH: pH 11.4 (gray line), pH 8.8 (light blue), pH 6.9 (pink), pH 5.8 (dark blue), pH 4.0 (yellow), pH 2.98 (green), pH 1.98 (red) and pH 1.05 (black). (b) The ellipticity at 220 nm plotted as a function of pH for amyloid β peptide. The continuous line represents a sigmoidal fit to the data.

force–distance curves corresponding to different pH values are shown in Figure 5(a)–(d). The distribution histograms of rupture forces are shown as insets in the upper right corner of the force–distance plot. A typical force curve obtained at pH 9.8 is presented in Figure 5(a). The mean interaction force value was ∼50 pN. The same small value of the interaction force was obtained until the pH reached 3.7, where the mean value for the interaction force was 850 pN (Figure 5(b)); that is almost 20 times higher than the value obtained at higher pH values. However, further decrease of pH leads to a decrease of the interaction force (pH 2; Figure 5(c)), which drops more upon further decrease of pH (pH 1.0; Figure 5(d)).

The dependence of the mean rupture force values on pH is shown in Figure 6. Different symbols represent independently acquired data sets. The rupture force is small (∼50 pN) and almost constant at alkaline, neutral and slightly acidic pH values. The force grows fast below pH 5.6, reaches a maximum at pH 3.7 and then drops significantly at very acidic pH values. Such a sharp pH-dependence of the rupture forces suggests that a decrease in pH induces considerable conformational changes in α-synuclein. The data for control experiments in which α-synuclein molecules immobilized on the surface were probed by the tip with no peptide bound are shown on the same graph with red triangles. This interaction

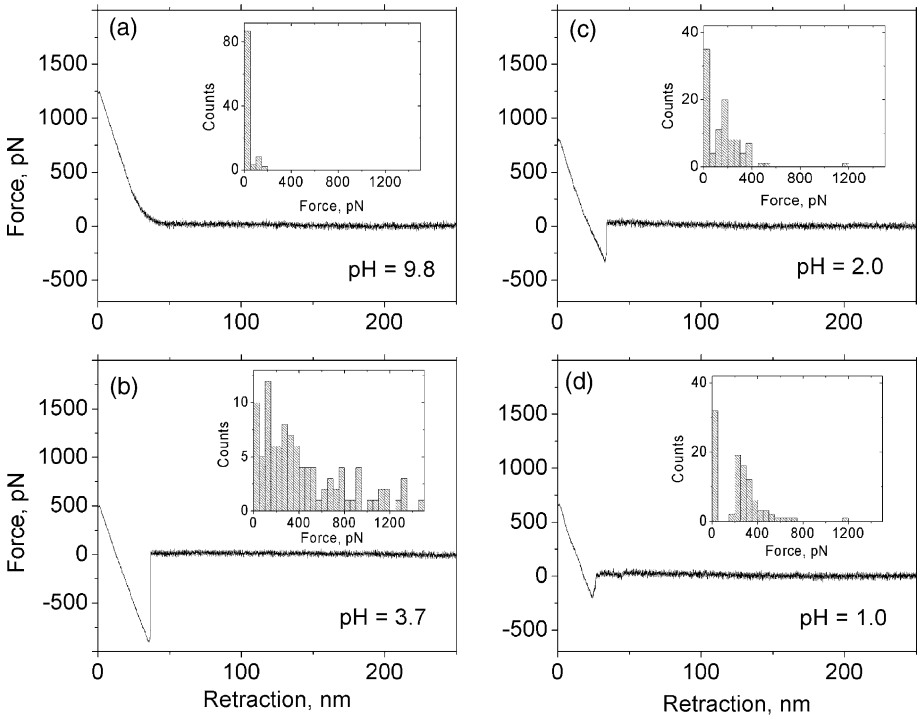

Figure 5. Force spectroscopy experiments for α-synuclein. Typical force curves and histograms summarizing all force curves taken at (a) pH 9.8, (b) pH 3.7, (c) pH 2.0, and (d) pH 1.0.

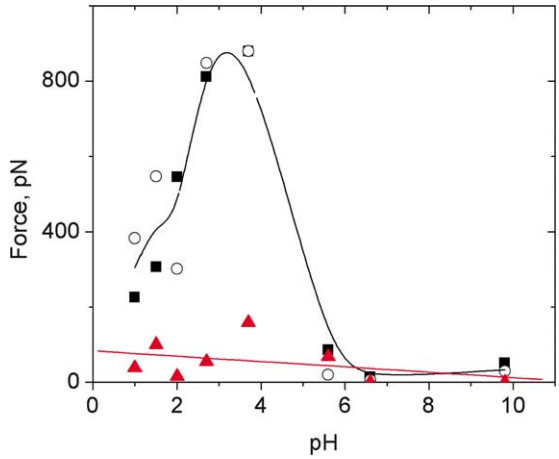

Figure 6. The mean pull-off force plotted as a function of pH for two independent trials (filled squares and open circles) for α-synuclein. The continuous black line represents a smooth fit to the average of the two data sets. Triangles show the results of control experiments for α-synuclein immobilized on the surface and the AFM tip terminated with OH groups. The continuous line represents a smooth fit to the data points.

remains very small and almost constant over the entire range of pH values.

Similar to our studies with amyloid β peptide, we verified the assumption that dramatic changes in the pulling force correlate with changes in protein structure using far-UV CD spectroscopy and 8-anilino-1-naphthalene sulfonic acid (ANS) fluorescence measurements. The same protein batch was used, and the CD spectra recorded over a broad range of pH values are shown in Figure 7(a). The far-UV CD spectra measured over the range between pH 11.4 and pH 5.8 are very similar, and show characteristic minima in the vicinity of 200 nm and the absence of bands around 210–230 nm; i.e. their shape is typical of an essentially unfolded polypeptide chain. Thus, these spectra indicate little, if any, α-helix or β-sheet structure present in α-synuclein.

The pH-dependence of the force spectroscopy and CD data suggest that α-synuclein should aggregate quickly at acidic pH. Indeed, typically, it takes a few weeks or months to obtain the fibrils at neutral pH,[44] whereas the rate of fibril formation is dramatically faster at acidic pH.[17,32] Based on the dependence of the rupture force data on pH, we were able to obtain, with a high yield, fibrils as long as several micrometers during several days of incubation without agitation. Figure S3 shows images of filaments obtained after seven days incubation at acidic pH (2.7) and elevated temperature (57 °C). In addition to protofilaments characterized by a small height or diameter (fibril 1), thick and twisted fibrils (e.g. fibril 2) are the most abundant morphologies under these conditions. A common feature of the sample obtained at these conditions is the formation of frayed ends. One of them is indicated in Supplementary Data, Figure S3 with an arrowhead. These images support the model of the fibrils as a bundle formed by thin protofilaments.[45] Note that the bundle-type model is also consistent with the structure of insulin fibrils proposed very recently.[46]

Lysozyme

The force spectroscopy assay for monitoring interprotein interaction leading to protein aggregation was tested on lysozyme aggregation, which has been documented recently.[47–49] In contrast to the

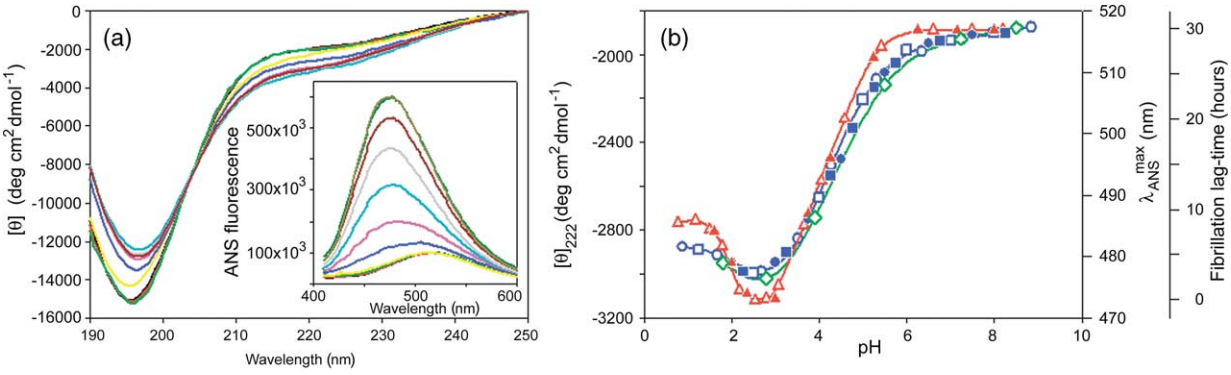

Figure 7. Optical spectroscopy data for α-synuclein. (a) Far-UV CD spectra as a function of pH. The values were pH 8.9 (black line), pH 7.3 (red line), pH 6.4 (green line), pH 5.3 (yellow line), pH 4.3 (blue line), pH 3.5 (pink line), pH 2.7 (cyan line), pH 1.7 (gray line) and pH 0.9 (dark red line). The inset represents ANS fluorescence spectra measured at the following values: pH 8.2 (black line), pH 7.5 (red line), pH 6.6 (green line), pH 5.4 (yellow line), pH 4.6 (blue line), pH 4.0 (pink line), pH 3.7 (cyan line), pH 3.1 (gray line), pH 2.8 (dark red line), pH 2.5 (dark green line), and pH 2.3 (dark yellow line). (b) The dependence of far-UV CD (blue line, circles and squares) and ANS fluorescence spectra (red line and triangles) on pH. The results of the initial titration (decrease in pH) and reverse experiments (increase in pH) are presented as open and filled symbols, respectively. For far-UV CD and fluorescence measurements, the cell pathlength was 0.1 mm and 10 mm, respectively. Measurements were carried out at 20 °C. The protein concentration was 0.1 mg/ml (circles) 1.0 mg/ml (squares) and 0.01 mg/ml (triangles). Data on the pH effect on the lag time of α-synuclein fibrillation (green line and diamonds) are shown for comparison.

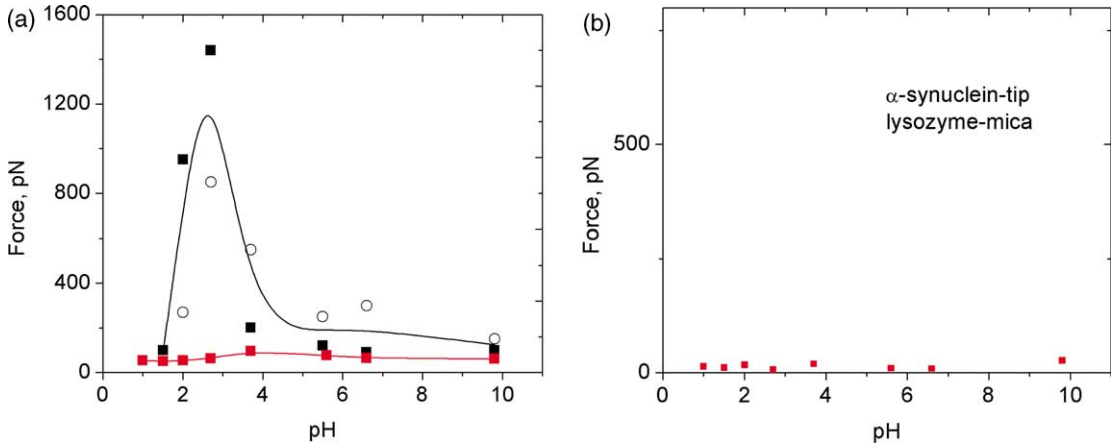

Figure 8. The mean pull-off force plotted as a function of pH. 9. (a) The data for two independent trials (squares and open circles) for lysozyme–lysozyme interaction. The continuous line represents a smooth fit to the average of the two data sets. Color symbols and a red curve correspond to the mean pull-off force plotted as a function of pH for lysozyme immobilized on the surface and an untreated AFM tip. (b) The mean pull-off force plotted as a function of pH for lysozyme immobilized on the surface and α-synuclein bound to the AFM tip.

natively unfolded Aβ and α-synuclein, lysozyme is a well-folded globular protein. The plot in Figure 8(a) summarizes the force spectroscopy results obtained at different pH values. This Figure shows that intermolecular interactions for lysozyme increase dramatically at pH below 4, and at pH 3 reach a value about ten times higher than the forces obtained under neutral conditions. Interestingly, the interaction drops sharply at pH 1.5. Control experiments with the use of a bare tip showed no pH-dependent interaction (red squares on the same plot). Additional control experiments, in which interaction between α-synuclein molecules immobilized on the surface and lysozyme molecules bound to the AFM tip did not reveal pH-dependent interaction between these proteins (Figure 8(b)).

To correlate the pH-induced changes in the pulling forces with the protein conformational changes, the pH-dependence of the lysozyme CD spectra was obtained. The results of this analysis are shown in Figure 9(a). The far-UV CD spectra measured over the pH range between 10.0 and 3.8 are very similar, and their shape is typical of a well-folded, mostly α-helical protein; i.e. these spectra possess a characteristic minimum in the vicinity of 208 nm and an intensive band around 222 nm. The decrease in pH between 3.8 and 2.0 brings about insignificant spectral changes, with the intensity of the 208 nm band being invariant, and the intensity of the 222 nm band being reduced by ~12–15%. These changes in far-UV CD spectra indicate a small but reproducible reduction in α-helical structure. The dependence of ellipticity values at 222 nm on pH is shown in Figure 9(b). These data clearly indicate the structural transition at acidic pH and the range of these changes coincides with a dramatic increase of the protein–protein interaction forces shown in Figure 8(a).

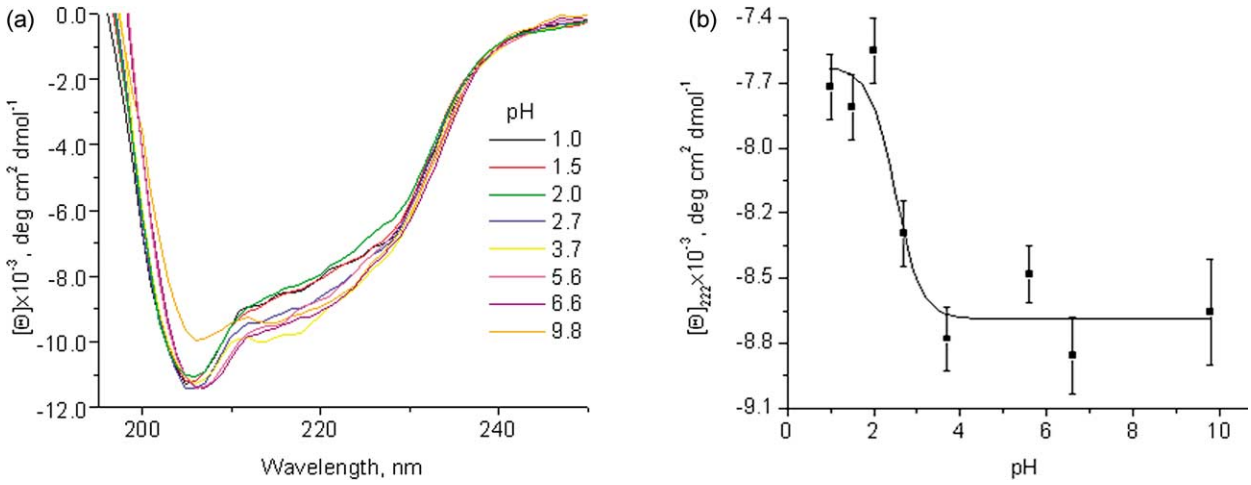

Figure 9. Conformational analysis of lysozyme at different pH values. (a) Far-UV CD spectra of lysozyme measured at different pH values. The concentration of lysosyme was 2 mg/ml, 0.15 M NaCl, cuvette pathlength 1 mm. (b) Dependence of far-UV CD spectrum of lysozyme on pH measured as changes in $[\theta]_{222}$.

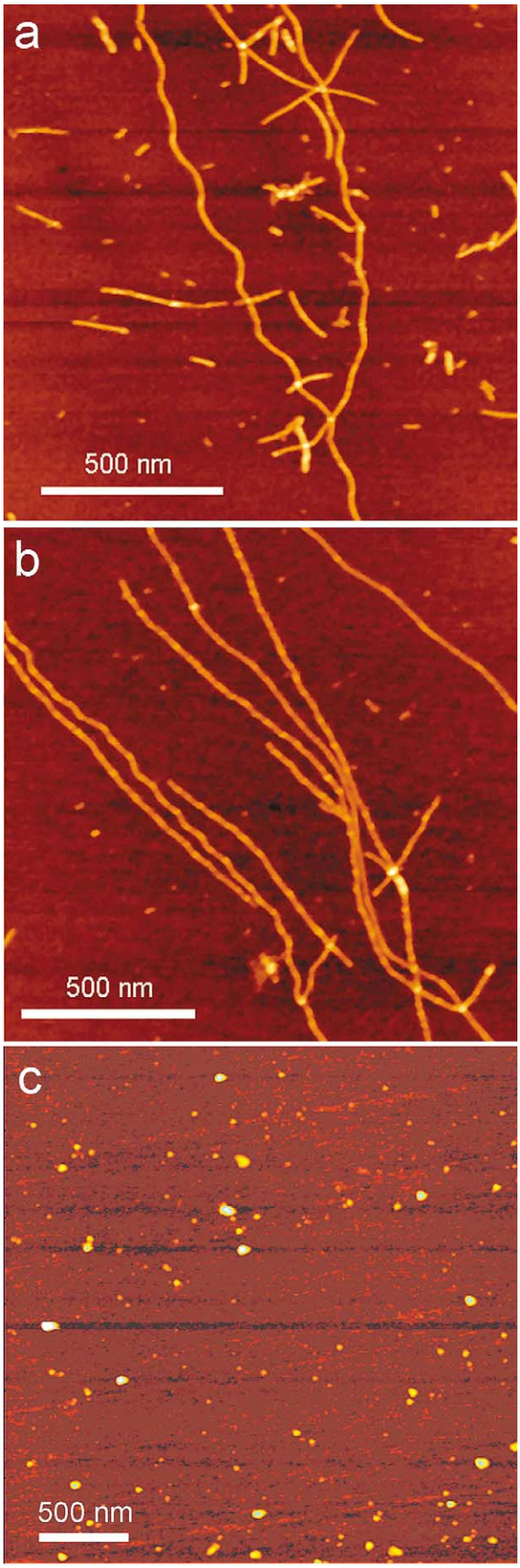

On the basis of these findings and earlier observations that at acidic pH the temperature-denatured lysozyme is prone to aggregate,[36,50] we performed experiments on growing the fibrils. The protein solution (10 mg/ml) was incubated at 57 °C in different buffers at pH 2.0, pH 2.7 and pH 3.7. The image of the sample prepared at pH 2.0 is shown in Figure 10(a). Fibrils are seen easily, although the sample prepared under these conditions is characterized by the appearance of short fibrils and small globular aggregates. The sample prepared at pH 2.7 has predominately fibrillar morphology (Figure 10(b)) with fibrils as long as several micrometers. The incubation at pH 3.7 did not lead to the formation of fibrils or large aggregates (Figure 10(c)).

Discussion

The AFM results (Figures 2, 6 and 8(a)) show that at acidic pH all three proteins studied here adopt conformations that lead to a dramatic increase in the interprotein interaction. Furthermore, the pH-dependence is sharp, suggesting that the conformational transition is highly cooperative. Importantly, the pH-dependence remains the same, regardless of the direction of the change in pH value, suggesting that the conformational transition is reversible. The AFM imaging studies showed that proteins in these conformations form aggregates with the fibril morphology rather easily. Although the fact that protein aggregation is facilitated at acidic pH has been reported, the finding that the transition into the aggregation-prone conformation is accompanied by a dramatic and cooperative increase in the interprotein interaction has not been reported before. The nature of this conformation cannot be retrieved from the AFM data, but parallel CD studies showed that the structural transition into an aggregation-prone conformation is characterized by the extensive formation of the β-sheet geometry that is in line with the well-documented fact that the formation of β-sheets is a key step in protein misfolding followed by spontaneous aggregation.

Control experiments for α-synuclein and lysozyme (Figures 6 and 8(a)) showed no interaction between the protein and the uncoated tip (bare or terminated with OH groups) over the entire range of pH values. Importantly, control experiments revealed that there is no pH-dependent interaction between these two proteins (α-synuclein and lysozyme, Figure 8(b)). In this regard, control data for amyloid β peptide indicating a monotonous increase of unbinding forces with lowering

Figure 10. AFM images of fibrils formed by lysozyme at different pH values: (a) pH 2, (b) pH 2.7 and (c) pH 3.7. The samples were deposited onto an APS mica surface.[26] Images were acquired in air with MM AFM operating in tapping mode.

pH (Figure 3) is quite surprising. However, this effect can be understood if the adhesion between various surfaces is taken into account. Strong adhesion effects between various surfaces have been studied systematically.[51] It has been shown that adhesion forces can be as large as dozens of nN for the surfaces terminated with amines (mica and silicon nitride functionalized with aminosilane). We used glycine to quench unreacted glutaraldehyde groups, and the adhesion forces between glycine residues immobilized on glutaraldehyde-terminated surfaces were relatively large too. The rupture forces increased monotonously in the range of pH between 1 and 10, reaching 1.9 nN at pH 1 (data not shown). This short-range, non-specific interaction can be screened by adding a layer of bulky molecules. Indeed, coating the surface with α-synuclein or lysozyme decreased the adhesion forces to the background level, allowing us to measure specific protein–protein interactions. Very likely, due to its small size, amyloid β peptide is not able to screen short-range surface–surface interactions efficiently; therefore, a monotonous increase of adhesion forces with decreasing pH was observed. However, the rupture force values were smaller than those observed in the case of glycine.

The comparison of the force spectroscopy data for amyloid β peptide (Figure 2) and α-synuclein (Figure 6) reveals rather strong interaction for amyloid β peptide before the structural transition range, even at neutral pH values. These data suggest that the formation of misfolded conformations of amyloid β peptide is not a rare event; presumably, these conformations exist intermittently and may lead to peptide aggregation under a variety of conditions. This interpretation is in line with the fact that amyloid β peptide aggregates under physiological conditions, so the formation of oligomers is a typical behavior of this protein. However, we should keep in mind that pathways for amyloid β peptide aggregation at neutral and acidic pH could be different,[12] suggesting that misfolded conformations stabilized under these conditions could be different too. At the same time, α-synuclein shows very weak interaction at neutral pH, suggesting that such conditions are not favorable for aggregation of this protein. This conclusion also correlates well with slow aggregation kinetics of α-synuclein. The pull-off forces for each set of experimental conditions corresponding to misfolded conformations (below the transition point) vary in a rather broad range. This effect can be explained partially by dynamic features of misfolded protein conformations or even an existing set of misfolded conformations. The latter hypothesis is supported by a complex and very broad (Figure 2(e)) or even bimodal (Figure 2(f)) distribution of pulling forces. However, additional experimental data are required to validate this hypothesis.

The pH-dependence data (see Figures 3, 6 and 9) are reminiscent of melting profiles;[52] therefore, we characterized each pH-dependence curve with two parameters, the transition point, $pH_{1/2}$, and the width of the transition, ΔpH (see the schema in Figure 3). $pH_{1/2}$ is the pH value corresponding to the middle of the pH-dependence profile and ΔpH was determined from the intersection points of the tangent to the curve at the transition point with upper and lower values of pulling forces. For lysozyme, the transition curve of which does not have an upper plateau (Figure 9), the maximum on the smoothed curve was taken as the upper level. The AFM results for the proteins are summarized in Table 1.

Table 1. Parameters of the transition curves for amyloid β peptide, α-synuclein and lysozyme (see Figures 2, 6, and 8)

	Amyloid β peptide	α-Synuclein	Lysozyme
$pH_{1/2}$	2.8	4.5	3.4
ΔpH	2	1.3	1.0

The $pH_{1/2}$ value varies for different proteins, reflecting the difference in amino acid composition. ΔpH is maximal for amyloid β peptide, indicating a relatively low cooperativity of structural transformations for amyloid β peptide in comparison with the longer proteins α-synuclein and lysozyme. Interestingly, pulling forces for the last two proteins drop after the first transition, suggesting that other conformational changes take place at extremely low pH values. This interpretation is supported by far-UV CD data for α-synuclein that indicate the change in the protein conformation. The drop in interprotein interaction is very abrupt for lysozyme. We hypothesize that existing disulfide bonds in the protein work as springs, pulling the protein from the aggregate-prone conformation as soon as the protonation conditions are not favorable for this conformation. However, additional experiments are required to validate this hypothetical model.

Traditionally, protein misfolding conformations are studied *via* the protein propensity to aggregate. Aggregation of proteins has been studied using various imaging techniques including AFM.[53] These imaging studies provide valuable information for understanding the morphology of aggregates that are formed, but do not explain why the aggregation happens or how it is linked to the protein conformation. The current investigation shows that the propensity of proteins to aggregate is a direct result of the increased attractive force between the molecules under these conditions. In addition, this study illustrates that AFM is a powerful technique that allows the probing of these interactions as a complement to the traditional use of this technique as an imaging tool. Importantly, the force spectroscopy approach for testing the propensity of protein to misfold and aggregate under specific conditions (reflected in the increase in the mean pull-off force) provides the results relatively quickly compared to traditional imaging methods. For example, AFM or EM imaging often involve lengthy observation of the aggregation process and typically take days or even several

months.[12] Importantly, force spectroscopy provides a quantitative measure for a protein's propensity to aggregate that can be useful for quantitative analysis of the misfolded conformation of a protein.

Conventional experimental approaches for protein conformational studies operate with an ensemble of molecules and cannot answer the question of whether the observed conformational changes occur in individual proteins or they are the characteristic features of proteins within oligomeric or polymeric aggregates. Anchoring the proteins to the surface prevents their aggregation, so the force spectroscopy approach is one of a few, or very likely the only, experimental approaches that allows uncoupling the protein misfolding and aggregation events. This approach was tested on three different proteins and shows that misfolding can occur at the level of individual protein molecules.

Although we studied the effect of pH on protein misfolding, a whole host of relevant solution conditions, including the presence of metal ions, various solvents, or potential therapeutic agents can be studied. In fact, the rate of fibril formation in α-synuclein was shown to be strongly dependent on numerous environmental factors.[16,17] Besides low pH and elevated temperature,[32] discussed here, the amyloidogenic partially folded conformation was shown to be stabilized in α-synuclein by the presence of several common pesticides and herbicides,[54–56] or metal ions,[56,57] or at moderate concentrations of trimethylamine-*N*-oxide,[58] or other organic solvents.[59] Importantly, under all these conditions, α-synuclein was shown to undergo significantly enhanced fibrillation. In contrast, fibril formation was considerably slowed or inhibited under conditions favoring formation of more folded conformations,[58,59] by stabilization of the fully unfolded form, e.g. by oxidation of its methionine residues,[60] or by stabilization of off-pathway oligomers *via* nitration of tyrosine residues.[61] Obviously, force spectroscopy can be used to analyze the effect of these and other factors on protein misfolding and interprotein interactions. These studies are in progress.

We used a rather simple immobilization approach for anchoring protein to the mica and to the tip surfaces *via* reaction of the protein amino groups with glutaraldehyde immobilized on the surfaces. Glutaraldehyde crosslinking capability is widely used for studying various protein–nucleic acids complexes. Recently, glutaraldehyde was applied for strong immobilization of chromatin on amino-terminated surfaces.[62] Here, we showed that the glutaraldehyde anchors are stable at a wide range of pH values, enabling us to probe protein–protein interactions at extreme pH values. The drawback of this anchoring approach is that the protein N-terminal amine groups are not the only anchoring sites in the protein. This procedure tethers certain of the peptide side-groups, e.g. lysine, to the surface, so the protein is anchored to the surface in a number of different ways. This means that protein molecules are oriented differently on the surfaces of mica and the tip, and they are oriented differently during probing the protein–protein interactions by the AFM tip. Different relative orientations may lead to variability in intermolecular interactions and thus to a broadening of the range of pulling forces measured in the AFM experiments. In addition, some anchored positions may interfere with the structural transition leading to the misfolded conformation of the protein. This is another source of broadening in the distribution pattern of pulling forces. However, our control experiments showed that glutaraldehyde-immobilized Aβ peptide retains the antigen activity in interaction with anti-Aβ antibodies, suggesting that the effect, if any, of anchoring on the protein structure is not significant. In addition, the coincidence of the structural transition profiles of the proteins revealed by AFM for immobilized peptides and CD for molecules moving freely in solution suggests that the proposed immobilization procedure is appropriate for interprotein studies such as that reported here. Availability of procedures allowing one-point anchoring with the use of flexible polyethylene glycol linkers will ease the problems listed above, and will allow extraction of the thermodynamic parameters of the protein–protein interaction.[40] A large range of the change of the pull-off forces in the protein conformational transition range suggests that the technique has prospects for future applications. The development of novel immobilization procedures and approaches for quantitative analysis are the two major issues that need to be addressed for further understanding the protein misfolding phenomenon. These efforts are underway.

The data obtained for the pH-induced formation of aggregation-prone intermediates provide a new insight into properties of misfolded conformations for different proteins. We compare below the data for α-synuclein and lysozyme, the two proteins with different conformations at neutral pH. The far-UV CD spectra of natively unfolded α-synuclein (Figure 7(a)) reflect the pH-induced formation of ordered secondary structure. Furthermore, the inset to Figure 7(a) shows that a decrease in pH leads to a large blue shift of the ANS fluorescence maximum (from ~515 nm to ~475 nm, open triangles in Figure 7(a)), suggesting the pH-induced transformation of the natively unfolded α-synuclein to the partially folded and partially compact conformation.[32] Figure 7(b) illustrates that the pH-induced structural transitions detected by ANS fluorescence and CD occur simultaneously in a rather co-operative manner, suggesting formation of a partially folded conformation with an increased amount of ordered secondary structure and with affinity for ANS. Importantly, pH-induced transition from unfolded to partially folded conformation was shown to be completely reversible (Figure 7(b), open and filled symbols) and independent of protein concentration, suggesting that this partial folding is an intramolecular process.[32]

Figure 7(b) shows that decreasing the pH resulted in a very substantial acceleration of the kinetics of α-synuclein fibrillation (green symbols and lines). In other words, an excellent correlation between intramolecular conformational change and fibril formation has been established. This very important observation is consistent with the conclusion that the process of α-synuclein fibrillation is accelerated dramatically by the partial folding of the natively unfolded protein, suggesting that this intermediate is a key species on the fibril-forming pathway.[32]

The pH-induced structural changes in lysozyme are entirely different. CD data (Figure 10) show that a decrease in pH is accompanied by a minor (~12–15%) decrease in the α-helical content of this protein. Thermodynamic analysis of lysozyme using differential scanning microcalorimetry revealed that the decrease in pH from 4.0 to 1.5 was accompanied by a decrease in protein conformational stability, as T_d dropped from 78 °C to 47 °C.[63] At the same time, calorimetric,[63] and near-UV CD analyses[50] revealed that the native well-folded structure is sustained in lysozyme even at pH 1.5. This suggests that at pH 1.5, lysozyme, being destabilized, preserves a rigid tertiary structure, thermal unfolding of which is associated with a dramatic absorption of heat.[50,63] Thus, the decrease in pH from 4.0 to 1.5–2.0 leads to the destabilization of lysozyme, which is accompanied by a reduction in α-helical structure (see Figure 10). Interestingly, these minor conformational changes are accompanied by a dramatic change of the interprotein interactions responsible for spontaneous assembly of the protein in ordered fibril structures.

There is growing evidence indicating that protein misfolding and fibrillation is a widespread phenomenon that is not limited to proteins associated with so-called conformational disorders.[2,64–67] It is believed that protein misfolding represents a key primary event in the aggregation/fibrillation pathway. However, our knowledge about this fundamental phenomenon is very restricted, and the detailed analysis of protein misfolding is almost impossible using a set of conventional experimental approaches, as they provide information averaged over the ensemble of all conformations and forms existing in solution. This represents a real problem for the aggregating system, a complex heterogeneous mixture, which besides the differently folded/unfolded/misfolded monomeric species contains a wide variety of different oligomers and aggregates. In addition, aggregation and oligomerization are known to affect the protein conformation. Typically, it is difficult to avoid contribution of aggregates due to a high aggregation propensity of the misfolded conformations, and many conventional methods provide the information on protein conformation within aggregates. As a consequence, the vast majority of current studies dealing with protein misfolding and aggregation are, in fact, focused on analysis of structural consequences of protein aggregation rather than on analysis of the consequences of protein misfolding. Thus, our poor understanding of the protein misfolding is due to a lack of appropriate methods. The approach described here is capable of characterizing protein misfolded conformations and separating them from the aggregated forms. Our data show that under conditions facilitating protein aggregation, protein can adopt an alternative, misfolded conformation. This indicates that misfolding is an intramolecular conformation transition, which does not necessarily require interaction with another protein molecule(s). Overall, our study revealed that, at acidic pH, proteins undergo structural transition into conformations responsible for the dramatic increase in interprotein interaction and promoting the formation of protein aggregates. We believe that these novel findings have clear biological implications, and the application of the approach described might open new routes in the analysis and understanding of the protein misfolding phenomenon.

Materials and Methods

Amyloid β samples preparation

Lyophilized Aβ (1-40) was a generous gift from Alex Rohr (Sun Health Research Institute, Sun City, AZ). Aβ stock solutions were prepared using a modification of the protocol used by Chakrabartty and co-workers.[71] Lyophilized A-β (1-40) was dissolved in 6.0 M guanidine–HCl to a final concentration of 1 mg/ml. It was incubated at room temperature for 5 min, followed by immediate exchange of the buffer with 10 mM Na_2CO_3 (pH 9.8) using Microcon centrifugal filters. The stock solution was stored at −20 °C. Samples of amyloid β peptide for CD and fluorescence measurements were prepared by dissolving lyophilized protein in sterile 0.1 M NaOH in doubly deionized water (pH 10.9) for 20 min on ice, followed by neutralizing with the appropriate buffer. These solutions were either centrifuged at 14,000 rpm (16,863 *g*) for 10 min at 4 °C or airfuged (178,000 *g*) at 24 psi (1 psi ≈6.9 kPa) for 10 min to pellet any insoluble material.

α-Synuclein preparation

Wild-type human α-synuclein was expressed in *Escherichia coli* cell line BL21(DE3) transfected with pRK172/α-synuclein plasmid. Expression and purification of human recombinant α-synuclein and its mutants from *E. coli* were performed as described.[61] After the purification, protein solutions were dialyzed four times against doubly deionized water at 4 °C, lyophilized, and stored at −80 °C. Samples of α-synuclein for CD and fluorescence measurements were prepared by dissolving lyophilized protein in sterile 0.1 M NaOH in doubly deionized water (pH 10.9) for 20 min on ice, followed by neutralizing with the appropriate buffer. These solutions were either centrifuged at 14,000 rpm (16,863 *g*) for 10 min at 4 °C or airfuged (178,000 *g*) at 24 psi for 10 min to pellet any insoluble material. Protein concentrations were determined spectrophotometrically with an extinction coefficient $\varepsilon_{280\,nm}=5120\ M^{-1}\ cm^{-1}$. The atomic force

spectroscopy procedure was the same as that described above for amyloid β peptide. For the fibrils growth, α-synuclein was dissolved in 10 mM glycine–HCl buffer pH 2.7 with 150 mM NaCl added. The concentration of α-synuclein was ~1 mg/ml. The solution was incubated at 57 °C for seven to ten days without shaking.

Lysozyme fibril formation.

Chicken egg lysozyme (Sigma L-6876) was dissolved in 10 mM Hepes (pH 7.5) at a concentration of 1 mg/ml and stored at 4 °C for no longer than a week. Lysozyme fibrils were obtained during incubation of the protein at a concentration of 10 mg/ml at 57 °C in three different buffers: 70 mM KCl–HCl (pH 2.0), 80 mM NaCl; 70 mM glycine–HCl (pH 2.7), 80 mM NaCl; 10 mM sodium acetate buffer (pH 3.7), 140 mM NaCl. After ten days of incubation, the samples were imaged with AFM.

Protein immobilization on the mica surface and AFM cantilevers

Silicon nitride cantilevers (Oriented Twin Tips, Nanoprobes, Digital Instruments, Santa Barbara, CA) were cleaned in 95% (v/v) ethanol for 1 h followed by exposure to UV light 1 h.[68] Freshly cleaved mica and cleaned silicon nitride cantilevers were modified identically according to the following procedure. First, both were modified with 167 μM aminopropylsilatrane (APS) in water for 30 min, followed by a brief rinse with nanopure water and drying with argon as described.[69] Both were then immersed in 10% (v/v) glutaraldehyde in water for 1 h, followed by a brief rinse with nanopure water. Both were then incubated with protein in 20 mM PBS (pH 7.0), 150 mM NaCl for 1 h, followed by a brief rinse with nanopure water. The concentration of the protein was adjusted in a way that provided primarily single interaction force curves characteristic for the single-molecule event interaction events; for different proteins, this was in the range of 10–20 μg/ml. For this incubation, a 10 μl droplet of the protein solution was deposited on top of the mica in a humid environment to prevent evaporation, and the AFM tip was placed inside a 150 μl droplet of the protein solution. Finally, both the mica and the AFM tip were immersed in 10 mM glycine in 20 mM PBS (pH 7.0, 150 mM NaCl for 1 h to quench unreacted immobilized glutaraldehyde molecules followed by a brief rinse with nanopure water. Higher concentrations of glycine (250 mM) and incubation for 10 min was an alternative protocol used. The mica and the AFM tip were stored in 10 mM Na_2CO_3 (pH 9.8) at 4 °C for not less than 12 h. The latter procedure facilitates the dissociation of protein aggregates formed spontaneously in solution during the previous sample immobilization step (pH 7). In control experiments, either bare silicon nitride probes or probes terminated with OH groups (OH-terminated surfaces showed the smallest adhesion effects[51]) were used. The OH-terminated probes were obtained by treatment of the probes functionalized with APS and glutaraldehyde with 10 mM sodium borohydride in methanol. The mica and the probes surfaces terminated with glycine were prepared in the same way as the surfaces with immobilized protein, except that after treatment with glutaraldehyde both the mica and AFM tip were immersed in 10 mM glycine in 20 mM PBS (pH 7.0), 150 mM NaCl for 1 h followed by a brief rinse with nanopure water.

Force spectroscopy

Force curves were generated with a Nanoscope MultiMode AFM with IIIa controller with the use of the Picoforce module (Veeco Metrology, Inc, Santa Barbara, CA). The ramp size used was 250 nm with a 1 Hz frequency and an application force of less than 1 nN for all force curves acquired. Silicon nitride cantilevers with a nominal spring constant of 0.06 N/m were used. Spring constants for each cantilever were obtained using the thermal method *via* the Nanoscope software (version 6.1).[70] Extension and retraction curves were acquired systematically at approximately 100 locations on the surface, initially in 10 mM Na_2CO_3 buffer (pH 9.8), 150 mM NaCl. The buffers were exchanged sequentially in order of decreasing pH, and force curves at the same locations on the surface were acquired at each pH value. The other buffers used for Aβ peptide, in the order used, were 20 mM PBS (pH 7.0), 10 mM sodium acetate (pH 5.1), 10 mM sodium acetate (pH 3.7, 20 mM PBS (pH 2.0), and 100 mM HCl (pH 1.0). NaCl was added to each buffer to a final concentration of 150 mM, with the exception of the 100 mM HCl, to which NaCl was added to a final concentration of 70 mM. This allowed for similar salt concentrations for each of the buffers used. For α-synuclein and lysozyme proteins, the buffers were slightly different. They were 100 mM sodium phosphate (pH 6.6), 100 mM sodium phosphate (pH 5.6), 10 mM sodium acetate (pH 3.7), 70 mM glycine–HCl (pH 2.7), 70 mM KCl–HCl (pH 2.0), 100 mM KCl–HCl (pH 1.5), 150 mM KCl–HCl (pH 1.0) with NaCl added in each buffer to the final ionic strength of 150 mM. Each buffer was allowed to incubate with the tip and surface in the liquid cell for at least 5 min before the acquisition of any force curves. The mean values for rupture forces obtained at selected pH values were calculated over entire data sets without approximation of the set with a particular function (Gaussian or Poisson distributions).

Circular dichroism spectroscopy

CD spectra were obtained on an AVIV 60DS spectrophotometer (Lakewood, NJ) using concentrations of Aβ of 1.0 mg/ml. Spectra were recorded in 0.01 cm cells from 250–190 nm with a step-size of 1.0 nm, a bandwidth of 1.5 nm, and an averaging time of 10 s. For all spectra, an average of five scans was obtained. CD spectra of the appropriate buffers were recorded and subtracted from the protein spectra.

Acknowledgements

We thank L. Shlyakhtenko for useful comments at all stages of the work, A. Roher (Sun Health Research Institute, Sun City, AZ) for providing us with the amyloid β peptide sample and anonymous reviewers for valuable and stimulating critical comments. The work was supported by grants from Arizona Disease Research Commission (ADCRC), M. J. Fox Parkinson's Foundation and NIH (1PN1EY016593-01) (all to Y.L.L.), and by INTAS 2001-2347 grant to V.N.U.

Supplementary Data

Supplementary data associated with this article can be found at 10.1016/j.jmb.2005.10.012

References

1. Kelly, J. W. (1998). The alternative conformations of amyloidogenic proteins and their multi-step assembly pathways. *Curr. Opin. Struct. Biol.* **8**, 101–106.
2. Dobson, C. M. (1999). Protein misfolding, evolution and disease. *Trends Biochem. Sci.* **24**, 329–332.
3. Bellotti, V., Mangione, P. & Stoppini, M. (1999). Biological activity and pathological implications of misfolded proteins. *Cell Mol. Life Sci.* **55**, 977–991.
4. Uversky, V. N., Talapatra, A., Gillespie, J. R. & Fink, A. L. (1999). Protein deposits as the molecular basis of amyloidosis. I. Systemic amyloidoses. *Med. Sci. Monitor*, **5**, 1001–1012.
5. Uversky, V. N., Talapatra, A., Gillespie, J. R. & Fink, A. L. (1999). Protein deposits as the molecular basis of amyloidosis. II. Localized amyloidosis and neurodegenerative disorders. *Med. Sci. Monitor*, **5**, 1238–1254.
6. Rochet, J. C. & Lansbury, P. T., Jr (2000). Amyloid fibrillogenesis: themes and variations. *Curr. Opin. Struct. Biol.* **10**, 60–68.
7. Uversky, V. N. & Fink, A. L. (2004). Conformational constraints for the amyloid fibrillation: the importance of being unfolded. *Biochim. Biophys. Acta*, **1698**, 131–153.
8. Dobson, C. M. (2003). Protein folding and misfolding. *Nature*, **426**, 884–890.
9. Dobson, C. M. (2004). Principles of protein folding, misfolding and aggregation. *Semin. Cell Dev. Biol.* **15**, 3–16.
10. Bucciantini, M., Giannoni, E., Chiti, F., Baroni, F., Formigli, L., Zurdo, J. *et al*. (2002). Inherent toxicity of aggregates implies a common mechanism for protein misfolding diseases. *Nature*, **416**, 507–511.
11. Hardy, J. & Selkoe, D. J. (2002). The amyloid hypothesis of Alzheimer's disease: progress and problems on the road to therapeutics. *Science*, **297**, 353–356.
12. Stine, W. B., Jr, Dahlgren, K. N., Krafft, G. A. & LaDu, M. J. (2003). *In vitro* characterization of conditions for amyloid-beta peptide oligomerization and fibrillogenesis. *J. Biol. Chem.* **278**, 11612–11622.
13. Petkova, A. T., Ishii, Y., Balbach, J. J., Antzutkin, O. N., Leapman, R. D., Delaglio, F. & Tycko, R. (2002). A structural model for Alzheimer's beta-amyloid fibrils based on experimental constraints from solid state NMR. *Proc. Natl Acad. Sci. USA*, **99**, 16742–16747.
14. Tycko, R. (2003). Insights into the amyloid folding problem from solid-state NMR. *Biochemistry*, **42**, 3151–3159.
15. Tycko, R. & Ishii, Y. (2003). Constraints on supramolecular structure in amyloid fibrils from two-dimensional solid-state NMR spectroscopy with uniform isotopic labeling. *J. Am. Chem. Soc.* **125**, 6606–6607.
16. Uversky, V. N., Li, J., Souillac, P., Millett, I. S., Doniach, S., Jakes, R. *et al*. (2002). Biophysical properties of the synucleins and their propensities to fibrillate: inhibition of alpha-synuclein assembly by beta- and gamma-synucleins. *J. Biol. Chem.* **277**, 11970–11978.
17. Uversky, V. N. (2003). A protein-chameleon: conformational plasticity of alpha-synuclein, a disordered protein involved in neurodegenerative disorders. *J. Biomol. Struct. Dynam.* **21**, 211–234.
18. Trojanowski, J. Q. (2003). Rotenone neurotoxicity: a new window on environmental causes of Parkinson's disease and related brain amyloidoses. *Expt. Neurol.* **179**, 6–8.
19. Trojanowski, J. Q. & Lee, V. M. (2003). Parkinson's disease and related alpha-synucleinopathies are brain amyloidoses. *Ann. NY Acad. Sci.* **991**, 107–110.
20. Lundvig, D., Lindersson, E. & Jensen, P. H. (2005). Pathogenic effects of alpha-synuclein aggregation. *Brain Res. Mol. Brain Res.* **134**, 3–17.
21. Bennett, M. C. (2005). The role of alpha-synuclein in neurodegenerative diseases. *Pharmacol. Ther.* **105**, 311–331.
22. Pountney, D. L., Voelcker, N. H. & Gai, W. P. (2005). Annular alpha-synuclein oligomers are potentially toxic agents in alpha-synucleinopathy. Hypothesis. *Neurotox. Res.* **7**, 59–67.
23. Volles, M. J. & Lansbury, P. T., Jr (2003). Zeroing in on the pathogenic form of alpha-synuclein and its mechanism of neurotoxicity in Parkinson's disease. *Biochemistry*, **42**, 7871–7878.
24. Dedmon, M. M., Christodoulou, J., Wilson, M. R. & Dobson, C. M. (2005). Heat shock protein 70 inhibits alpha-synuclein fibril formation *via* preferential binding to prefibrillar species. *J. Biol. Chem.* **280**, 14733–14740.
25. Murray, I. V., Giasson, B. I., Quinn, S. M., Koppaka, V., Axelsen, P. H., Ischiropoulos, H. *et al*. (2003). Role of alpha-synuclein carboxy-terminus on fibril formation *in vitro*. *Biochemistry*, **42**, 8530–8540.
26. Kessler, J. C., Rochet, J. C. & Lansbury, P. T., Jr (2003). N-terminal repeat domain of alpha-synuclein inhibits beta-sheet and amyloid fibril formation. *Biochemistry*, **42**, 672–678.
27. Hoyer, W., Antony, T., Cherny, D., Heim, G., Jovin, T. M. & Subramaniam, V. (2002). Dependence of alpha-synuclein aggregate morphology on solution conditions. *J. Mol. Biol.* **322**, 383–393.
28. Conway, K. A., Rochet, J. C., Bieganski, R. M. & Lansbury, P. T., Jr (2001). Kinetic stabilization of the alpha-synuclein protofibril by a dopamine-alpha-synuclein adduct. *Science*, **294**, 1346–1349.
29. Conway, K. A., Lee, S. J., Rochet, J. C., Ding, T. T., Harper, J. D., Williamson, R. E. & Lansbury, P. T., Jr (2000). Accelerated oligomerization by Parkinson's disease linked alpha-synuclein mutants. *Ann. NY Acad. Sci.* **920**, 42–45.
30. Conway, K. A., Lee, S. J., Rochet, J. C., Ding, T. T., Williamson, R. E. & Lansbury, P. T., Jr (2000). Acceleration of oligomerization, not fibrillization, is a shared property of both alpha-synuclein mutations linked to early-onset Parkinson's disease: implications for pathogenesis and therapy. *Proc. Natl Acad. Sci. USA*, **97**, 571–576.
31. Wood, S. J., Wypych, J., Steavenson, S., Louis, J. C., Citron, M. & Biere, A. L. (1999). alpha-synuclein fibrillogenesis is nucleation-dependent. Implications for the pathogenesis of Parkinson's disease. *J. Biol. Chem.* **274**, 19509–19512.
32. Uversky, V. N., Li, J. & Fink, A. L. (2001). Evidence for a partially folded intermediate in alpha-synuclein fibril formation. *J. Biol. Chem.* **276**, 10737–10744.

33. Pepys, M. B., Hawkins, P. N., Booth, D. R., Vigushin, D. M., Tennent, G. A., Soutar, A. K. *et al*. (1993). Human lysozyme gene mutations cause hereditary systemic amyloidosis. *Nature*, **362**, 553–557.
34. Morozova-Roche, L. A., Zurdo, J., Spencer, A., Noppe, W., Receveur, V., Archer, D. B. *et al*. (2000). Amyloid fibril formation and seeding by wild-type human lysozyme and its disease-related mutational variants. *J. Struct. Biol.* **130**, 339–351.
35. Malisauskas, M., Ostman, J., Darinskas, A., Zamotin, V., Liutkevicius, E., Lundgren, E. & Morozova-Roche, L. A. (2005). Cytotoxic effect of transient amyloid oligomers from common equine lysozyme *in vitro*: does it imply innate amyloid toxicity? *J. Biol. Chem.* **280**, 6269–6275.
36. Arnaudov, L. & de Vries, R. (2005). Thermally induced fibrilar aggregation of hen egg white lysozyme. *Biophys. J.*, ?????.
37. Goers, J., Permyakov, S. E., Permyakov, E. A., Uversky, V. N. & Fink, A. L. (2002). Conformational prerequisites for alpha-lactalbumin fibrillation. *Biochemistry*, **41**, 12546–12551.
38. Dufrene, Y. F. (2003). Recent progress in the application of atomic force microscopy imaging and force spectroscopy to microbiology. *Curr. Opin. Microbiol.* **6**, 317–323.
39. Limansky, A. P., Shlyakhtenko, L. S., Schaus, S., Henderson, E. & Lyubchenko, Y. L. (2002). Amino-modified probes for atomic force microscopy. *Probe Microsc.* **2**, 227–234.
40. Riener, C. K., Stroh, C. M., Ebner, A., Gall, A. A., Klampfl, C., Romanin, C. *et al*. (2003). A simple test system for single molecule recognition force microscopy. *Anal. Chim. Acta*, **479**, 59–75.
41. Zhang, Q., Powers, E. T., Nieva, J., Huff, M. E., Dendle, M. A., Bieschke, J. *et al*. (2004). Metabolite-initiated protein misfolding may trigger Alzheimer's disease. *Proc. Natl Acad. Sci. USA*, **101**, 4752–4757.
42. Lyubchenko, Y. L. & Shlyakhtenko, L. S. (1997). Visualization of supercoiled DNA with atomic force microscopy *in situ*. *Proc. Natl Acad. Sci. USA*, **94**, 496–501.
43. Shlyakhtenko, L. S., Gall, A. A., Weimer, J. J., Hawn, D. D. & Lyubchenko, Y. L. (1999). Atomic force microscopy imaging of DNA covalently immobilized on a functionalized mica substrate. *Biophys. J.* **77**, 568–576.
44. Shtilerman, M. D., Ding, T. T. & Lansbury, P. T., Jr (2002). Molecular crowding accelerates fibrillization of alpha-synuclein: could an increase in the cytoplasmic protein concentration induce Parkinson's disease? *Biochemistry*, **41**, 3855–3860.
45. Serpell, L. C. (2000). Alzheimer's amyloid fibrils: structure and assembly. *Biochim. Biophys. Acta*, **1502**, 16–30.
46. Jimenez, J. L., Nettleton, E. J., Bouchard, M., Robinson, C. V., Dobson, C. M. & Saibil, H. R. (2002). The protofilament structure of insulin amyloid fibrils. *Proc. Natl Acad. Sci. USA*, **99**, 9196–9201.
47. Canet, D., Last, A. M., Tito, P., Sunde, M., Spencer, A., Archer, D. B. *et al*. (2002). Local cooperativity in the unfolding of an amyloidogenic variant of human lysozyme. *Nature Struct. Biol.* **9**, 308–315.
48. De Felice, F. G., Vieira, M. N., Meirelles, M. N., Morozova-Roche, L. A., Dobson, C. M. & Ferreira, S. T. (2004). Formation of amyloid aggregates from human lysozyme and its disease-associated variants using hydrostatic pressure. *FASEB J.* **18**, 1099–1101.
49. Frare, E., Polverino De Laureto, P., Zurdo, J., Dobson, C. M. & Fontana, A. (2004). A highly amyloidogenic region of hen lysozyme. *J. Mol. Biol.* **340**, 1153–1165.
50. Babu, K. R. & Bhakuni, V. (1997). Ionic-strength-dependent transition of hen egg-white lysozyme at low pH to a compact state and its aggregation on thermal denaturation. *Eur. J. Biochem.* **245**, 781–789.
51. Vezenov, D. V., Noy, A., Rozsnyai, L. F. & Lieber, C. M. (1997). Force titrations and ionization state sensitive imaging of functional groups in aqueous solutions by chemical force microscopy. *J. Am. Chem. Soc.* **119**, 2006–2015.
52. Razlutskii, I. V., Shlyakhtenko, L. S. & Lyubchenko, Y. L. (1988). The DNA melting profile is sensitive to point mutations (in Russian). *Biopolimery Kletka*, **4**, 357–361.
53. Khurana, R., Ionescu-Zanetti, C., Pope, M., Li, J., Nielson, L., Ramirez-Alvarado, M. *et al*. (2003). A general model for amyloid fibril assembly based on morphological studies using atomic force microscopy. *Biophys. J.* **85**, 1135–1144.
54. Uversky, V. N., Li, J. & Fink, A. L. (2001). Pesticides directly accelerate the rate of alpha-synuclein fibril formation: a possible factor in Parkinson's disease. *FEBS Letters*, **500**, 105–108.
55. Manning-Bog, A. B., McCormack, A. L., Li, J., Uversky, V. N., Fink, A. L. & Di Monte, D. A. (2002). The herbicide paraquat causes up-regulation and aggregation of alpha-synuclein in mice: paraquat and alpha-synuclein. *J. Biol. Chem.* **277**, 1641–1644.
56. Uversky, V. N., Li, J., Bower, K. & Fink, A. L. (2002). Synergistic effects of pesticides and metals on the fibrillation of alpha-synuclein: implications for Parkinson's disease. *Neurotoxicology*, **23**, 527–536.
57. Uversky, V. N., Li, J. & Fink, A. L. (2001). Metal-triggered structural transformations, aggregation, and fibrillation of human alpha-synuclein. A possible molecular NK between Parkinson's disease and heavy metal exposure. *J. Biol. Chem.* **276**, 44284–44296.
58. Uversky, V. N., Li, J. & Fink, A. L. (2001). Trimethylamine-*N*-oxide-induced folding of alpha-synuclein. *FEBS Letters*, **509**, 31–35.
59. Munishkina, L. A., Phelan, C., Uversky, V. N. & Fink, A. L. (2003). Conformational behavior and aggregation of alpha-synuclein in organic solvents: modeling the effects of membranes. *Biochemistry*, **42**, 2720–2730.
60. Uversky, V. N., Yamin, G., Souillac, P. O., Goers, J., Glaser, C. B. & Fink, A. L. (2002). Methionine oxidation inhibits fibrillation of human alpha-synuclein *in vitro*. *FEBS Letters*, **517**, 239–244.
61. Yamin, G., Glaser, C. B., Uversky, V. N. & Fink, A. L. (2003). Certain metals trigger fibrillation of methionine-oxidized alpha-synuclein. *J. Biol. Chem.* **278**, 27630–27635.
62. Wang, H., Bash, R., Yodh, J. G., Hager, G. L., Lohr, D. & Lindsay, S. M. (2002). Glutaraldehyde modified mica: a new surface for atomic force microscopy of chromatin. *Biophys. J.* **83**, 3619–3625.
63. Privalov, P. L. & Khechinashvili, N. N. (1974). A thermodynamic approach to the problem of stabilization of globular protein structure: a calorimetric study. *J. Mol. Biol.* **86**, 665–684.
64. Fandrich, M., Fletcher, M. A. & Dobson, C. M. (2001). Amyloid fibrils from muscle myoglobin. *Nature*, **410**, 165–166.
65. Pertinhez, T. A., Bouchard, M., Tomlinson, E. J., Wain, R., Ferguson, S. J., Dobson, C. M. & Smith, L. J. (2001). Amyloid fibril formation by a helical cytochrome. *FEBS Letters*, **495**, 184–186.

66. Dobson, C. M. (2001). Protein folding and its links with human disease. *Biochem. Soc. Symp.*, 1–26.
67. Uversky, V. N. & Fink, A. L. (2004). Conformational constraints for amyloid fibrillation: the importance of being unfolded. *Biochim. Biophys. Acta*, **1698**, 131–153.
68. Shlyakhtenko, L. S., Gall, A. A., Weimer, J. J., Hawn, D. D. & Lyubchenko, Y. L. (1999). Atomic force microscopy imaging of DNA covalently immobilized on a functionalized mica substrate. *Biophys. J.* **77**, 568–576.
69. Shlyakhtenko, L. S., Gall, A. A., Filonov, A., Cerovac, Z., Lushnikov, A. & Lyubchenko, Y. L. (2003). Silatrane-based surface chemistry for immobilization of DNA, protein–DNA complexes and other biological materials. *Ultramicroscopy*, **97**, 279–287.
70. Walters, D. A., Cleveland, J. P., Thomson, N. H. & Hansma, P. K. (1996). Short cantilevers for atomic force microscopy. *Rev. Sci. Instrum.* **67**, 3583–3590.
71. Huang, T. H., Yang, D. S. ., Plaskos, N. P., Go, S., Yip, C. M., Fraser, P. E. & Chakrabartty, L. A. (2000). Structural studies of soluble oligomers of the Alzheimer beta-amyloid peptide *J. Mol. Biol.* **297**, 73–87.

Edited by P. T. Lansbury Jr

(Received 28 December 2004; received in revised form 30 August 2005; accepted 6 October 2005)
Available online 2 November 2005